Prepared for submission to JHEP

Interference Effects in Higgs production through Vector Boson Fusion in the Standard Model and its Singlet Extension.

Alessandro Ballestrero[a] **and Ezio Maina**[a,b]

[a] *INFN, Sezione di Torino,*
Via Giuria 1, 10125 Torino, Italy
[b] *Dipartimento di Fisica, Università di Torino,*
Via Giuria 1, 10125 Torino, Italy

E-mail: ballestrero@to.infn.it, maina@to.infn.it

Abstract: Interference effects play an important role in Electroweak Physics. They are responsible for the restoration of unitarity al large energies. When, as is often the case, higher order corrections are only available for some particular subamplitude, interferences need to be carefully computed in order to obtain the best theoretical prediction. In the new proposal to estimate the total Higgs width from the off shell cross section, the interference between the Higgs signal and the background is essential. It has been recently pointed out in gluon fusion that whenever more than one neutral, $\mathcal{CP}$ even, scalars are present in the spectrum large cancellations can occur. We extend these studies to Vector Boson Scattering, examining interference effects in the Higgs sector in the Standard Model and its one Higgs Singlet extension.

Contents

1 Introduction

Now that a resonance has been dicovered at about 125 GeV [1, 2], the race is on to measure all its properties. All studies based on LHC Run I data are consistent with the hypothesis that the new particle is indeed the Standard Model Higgs boson. The mass is already known with an uncertainty of two per mill from the latest published analyses [3, 4] and the signal strengths $\mu^i = \sigma^i/\sigma^i_{SM}$, where i runs over the decay channnels, are known to about 10 to 20% [3, 5, 6]. There is still room for more complicated Higgs sectors but compatibility with experimental results is severely restricting their parameter space [7]. In Run II, larger luminosity and energy will provide more precise measurements of the characteristics of the new particle and extend the mass range in which other scalars can be searched for.

Lately, a lot of attention has been paid to the prospects of detailed studies of off-shell Higgs contributions. On the one hand, at large energies, Higgs exchange unitarizes processes like Vector Boson Scattering (VBS) and fermion pair annihilation to Vector Bosons which would otherwise diverge. On the other hand, the comparison of off-shell and peak cross sections can provide limits on the total width of the Higgs [8], exploiting the interference of the Higgs contribution with the rest of the amplitude and the different dependence on the Higgs couplings of the two terms. Both aspects are sensitive to BSM physics, both through direct production of new states and through their contributions in loops.

If additional neutral scalars are present in the physical spectrum, non trivial interference effects have been demonstrated in Gluon Gluon Fusion (GGF) processes [9–12].

It is quite natural to extend these studies to VBS which has been traditionally regarded as the ultimate testing ground of the ElectroWeak Symmetry Breaking mechanism. The ratio of the Higgs production cross section in Vector Boson Fusion (VBF) to the cross section in gluon fusion grows for larger Higgs masses and, as a consequence, the importance of VBF as a discovery channel for new scalar resonances of an extended Higgs sector increases. VBF is not affected by BSM physics through loops[13], therefore it can be argued that the limits it provides on the Higgs width are less model dependent than those obtained in GGF. It is well known that interference effects between Higgs exchange diagrams and all other ones are large in VBF. The interference between Higgs fields of different masses in VBS will also be present and modulate the cancellations which restore unitarity.

There is a widespread belief that accurate predictions for the production af a heavy Higgs can be obtained by computing $pp \to jjH$, possibly folded with a Breit-Wigner distribution in order to control the effects of the Higgs width, and then decaying H to the desired final state. The appeal of this point of view is that higher order ElectroWeak corrections to $pp \to jjH$ are available at NLO [14, 15] and QCD corrections are known almost exactly at NNLO [16, 17]. However there are large interference effects among Higgs exchange diagrams already in the SM and similar phenomena are to be expected between the SM like Higgs and its eventual heavier partner, producing non negligible modifications to the cross section and resonance shape of the latter.

Run II will certainly allow to study Vector Boson Fusion in greater detail than it was possible with the limited statistics collected in Run I.

Since the landscape of possible extensions of the SM Higgs sector is quite complicated, it makes sense to examine the simplest renormalizable enlargement, that is the one Higgs Singlet Model (1HSM). It introduces one additional real scalar field which is a singlet under all SM gauge groups. The 1HSM has been extensively investigated in the literature [9–12, 18–41]. Recently, a great deal of activity has concentrated on establishing the restrictions imposed on its parameter space by theoretical and experimental constraints [35, 36, 39, 41]; on interference effects between the two neutral Higgs fields and with the continuum [10–12] and on possible consequences on the determination of the Higgs width through a measurement of the off-shell Higgs cross section [9, 40], as proposed in ref. [8].

To the best of our knowledge, all analyses so far have resorted to a superposition of a VBF Higgs signal times decay sample to the continuum, ignoring interferences, since no public MC is available for VBS in the 1HSM. We have upgraded `PHANTOM` [42], allowing for the simulation of the 1HSM and more generally for the presence of two neutral scalars.

In this paper we apply this new tool to study interference effects in $pp \to jjl^+l^-l'^+l'^-$ and $pp \to jjl^+\bar{\nu}_l l'^-\nu_{l'}$ production, where both l and l' can be either an electron or a muon, $l \neq l'$. This is a case study rather then a complete analysis and we are aware that rates are expected to be small [43, 44]. A careful investigation of all channels, including the semileptonic ones and exploiting all techniques to identify vector bosons decaying hadronically will be required to assess the observability of the 1HSM through VBF in Run II and beyond.

2 The Singlet Extension of the Standard Model

In the following we consider the singlet extension of the SM in the notation of ref. [35]. A real $SU(2)_L \otimes U(1)_Y$ singlet, S, is introduced and the term:

$$\mathscr{L}_s = \partial^\mu S \partial_\mu S - \mu_1^2 \Phi^\dagger \Phi - \mu_2^2 S^2 + \lambda_1 (\Phi^\dagger \Phi)^2 + \lambda_2 S^4 + \lambda_3 \Phi^\dagger \Phi S^2. \tag{2.1}$$

is added to the SM Lagrangian, where Φ is the usual Higgs doublet. $\mathscr{L}_s$ is gauge invariant and renormalizable. A $\mathcal{Z}_2$ symmetry , $S \leftrightarrow -S$, which forbids additional terms in the potential is assumed. A detailed discussion of the 1HSM without $\mathcal{Z}_2$ symmetry can be found in refs. [20, 22, 34, 37, 38].

The neutral components of these fields can be expanded around their respective Vacuum Expectation Values:

$$\Phi = \begin{pmatrix} G^\pm \\ \dfrac{v_d + l^0 + iG^0}{\sqrt{2}} \end{pmatrix} \qquad S = \frac{v_s + s^0}{\sqrt{2}}. \tag{2.2}$$

The minimum of the potential is achieved for

$$\mu_1^2 = \lambda_1 v_d^2 + \frac{\lambda_3 v_s^2}{2}; \qquad \mu_2^2 = \lambda_2 v_s^2 + \frac{\lambda_3 v_d^2}{2}, \tag{2.3}$$

provided

$$\lambda_1, \lambda_2 > 0; \qquad 4\lambda_1\lambda_2 - \lambda_3^2 > 0\,. \tag{2.4}$$

The mass matrix can be diagonalized introducing new fields h and H:

$$h = l^0 \cos\alpha - s^0 \sin\alpha \qquad \text{and} \qquad H = l^0 \sin\alpha + s^0 \cos\alpha \tag{2.5}$$

with $-\frac{\pi}{2} < \alpha < \frac{\pi}{2}$.
The masses are

$$M_{h,H}^2 = \lambda_1\, v_d^2 + \lambda_2\, v_s^2 \mp |\lambda_1\, v_d^2 - \lambda_2\, v_s^2| \sqrt{1 + \tan^2(2\alpha)}\,, \quad \tan(2\alpha) = \frac{\lambda_3 v_d v_s}{\lambda_1 v_d^2 - \lambda_2 v_s^2}, \tag{2.6}$$

with the convention $M_H^2 > M_h^2$.

The Higgs sector in this model is determined by five independent parameters, which can be chosen as

$$m_h,\, m_H,\, \sin\alpha,\, v_d,\, \tan\beta \,\equiv\, v_d/v_s\,, \tag{2.7}$$

where the doublet VEV is fixed in terms of the Fermi constant through $v_d^2 = G_F^{-1}/\sqrt{2}$. Furthermore one of the Higgs masses is determined by the LHC measurement of 125.02 GeV. Therefore, three parameters of the model, M_H, $\sin\alpha$, $\tan\beta$, are at present undetermined.

The Feynman rules for the 1HSM have been derived using FeynRules [45, 46]. [1]

It should be mentioned that allowing a discrete symmetry to be spontaneously broken, as is the case in the simplified model considered here when the singlet field S has a non zero vacuum expectation value, will introduce potentially problematic cosmic domain walls [48–53]. These considerations, however have little bearing on the paper's main point.

For future reference, we report the expression of the tree level partial width for the decay of the heavy scalar into two light ones:

$$\Gamma(H \to hh) = \frac{e^2 M_H^3}{128\pi M_W^2 s_W^2} \left(1 - \frac{4M_h^2}{M_H^2}\right)^{\frac{1}{2}} \left(1 + \frac{2M_h^2}{M_H^2}\right)^2 s_\alpha^2 c_\alpha^2 \left(c_\alpha + s_\alpha \tan\beta\right)^2 \tag{2.8}$$

and those of the width of both scalars:

$$\Gamma_h = \Gamma^{SM}(M_h) c_\alpha^2, \qquad \Gamma_H = \Gamma^{SM}(M_H) s_\alpha^2 + \Gamma(H \to hh) \tag{2.9}$$

where $c_\alpha = \cos\alpha$, $s_\alpha = \sin\alpha$.

The strongest limits on the parameters of the 1HSM ref. [36, 39, 41] come from measurements of the coupling strengths of the light Higgs [3, 5–7], which dominate for small masses of the heavy Higgs, and from the contribution of higher order corrections to precision measurements, in particular to the mass of the W boson [36], which provides the tightest constraint for large M_H. The most precise result for the overall coupling strength of the Higgs boson from CMS [3] reads

$$\hat{\mu} = \hat{\sigma}/\sigma_{SM} = 1.00 \pm 0.13. \tag{2.10}$$

Therefore the absolute value of $\sin\alpha$ cannot be larger than about 0.4. This is in agreement with the limits obtained in ref. [36, 39, 41] which conclude that the largest possible value for the absolute value of $\sin\alpha$ is 0.46 for M_H between 160 and 180 GeV. This limit becomes slowly more stringent for increasing heavy Higgs masses reaching about 0.2 at $M_H = 700$ GeV.

3 New Features in PHANTOM

PHANTOM has been upgraded to allow for the presence of two neutral $\mathcal{CP}$ even scalars. The parameters which control how the Higgs sector is simulated, with masses and widths expressed in GeV, are:

- `rmh`: light Higgs mass. If `rmh` < 0 all light and heavy Higgs exchange diagrams are set to zero.
- `gamh`: light Higgs width. If `gamh` < 0 the width is computed internally following the prescription of ref. [54] and multiplied by $\cos^2\alpha$ if working in the 1HSM.

[1] The corresponding UFO file [47], which allows the simulation at tree level of any process in the model, can be downloaded from http://personalpages.to.infn.it/~maina/Singlet.

The parameter `i_singlet` selects whether `PHANTOM` performs the calculations in the SM (`i_singlet`=0) or in the 1HSM (`i_singlet`=1). If the 1HSM is selected the following inputs are required:

- `rmhh`: heavy Higgs mass. If `rmhh` < 0 all heavy Higgs exchange diagrams are set to zero.
- `rcosa`: the cosine of the mixing angle α.
- `tgbeta`: $\tan\beta$.
- `gamhh`: heavy Higgs width. If `gamhh` < 0 the width is computed internally following the prescription of ref. [54] and then multiplied by $\sin^2\alpha$. $\Gamma(H \to hh)$, eq.(2.8), is then added to the result.

Moreover the contribution of the Higgs exchange diagrams can be computed separately, both in the SM and in the 1HSM, setting the following flag:

- `i_signal`: if `i_signal` $= 0$ the full matrix element is computed.
  If `i_signal` > 0 only a set of Higgs exchange diagrams are evaluated at $\mathcal{O}(\alpha_{EM}^6)$:
  - `i_signal` $= 1$: s-channel exchange contributions.
  - `i_signal` $= 2$: all Higgs exchange contributions to VV scattering.
  - `i_signal` $= 3$: all Higgs exchange contributions to VV scattering plus the Higgsstrahlung diagrams with $h, H \to VV$.

4 Notation and details of the calculation

We are going to present results, at the 13 TeV LHC, for $pp \to jj\, l^+l^-l'^+l'^-$ and $pp \to jj\, l^+\bar{\nu}_l l'^-\nu_{l'}$ production, where $l(l') = e, \mu$, $l \neq l'$. We have identified the light Higgs h with the resonance discovered in Run I and set its mass to 125 GeV, concentrating on the scenario in which the heavy Higgs H is still undetected.

Samples of events have been generated with `PHANTOM` using CTEQ6L1 parton distribution functions [55]. The ratio of vacuum expectation values, $\tan\beta$, has been taken equal to 0.3 for $M_H = 600$ GeV and $M_H = 900$ GeV, and equal to 1.0 for $M_H = 400$ GeV. This corresponds, using eq.(2.8) for the $H \to hh$ width and ref. [54] for the SM Higgs width, to $\Gamma_H = 4.08$ GeV for $M_H = 400$ GeV, $s_\alpha = 0.3$; $\Gamma_H = 6.45$ GeV for $M_H = 600$ GeV and $s_\alpha = 0.2$; $\Gamma_H = 89.14$ GeV for $M_H = 900$ GeV and $s_\alpha = 0.4$.

The charged leptons are required to satisfy:

$$p_{Tl} > 20\,\text{GeV}, \qquad |\eta_l| < 3.0, \qquad m_{l^+l^-} > 20\,\text{GeV} \tag{4.1}$$

while the cuts on the jets are:

$$p_{Tj} > 20\,\text{GeV}, \qquad |\eta_j| < 6.5, \qquad m_{j_1j_2} > 400\,\text{GeV}, \qquad \Delta\eta_{j_1j_2} > 2.0. \tag{4.2}$$

For proceses with two charged leptons and two neutrinos in the final state we further impose:

$$\not{p}_T > 20\,\text{GeV}, \qquad |m_{bl^+\nu_l} - m_{top}| > 10\,\text{GeV}, \qquad |m_{\bar{b}l^-\bar{\nu}_l} - m_{top}| > 10\,\text{GeV}. \tag{4.3}$$

The latter requirement eliminates the large contribution from EW and QCD top production.

In the following we will discuss various sets of diagrams and different groups of processes, therefore, we introduce our naming convention. We split the amplitude A, for each process, as:

$$A = A_h + A_H + A_0, \tag{4.4}$$

where $A_{h/H}$ denote the set of diagrams in which a light/heavy Higgs is exchanged and A_0 the set of diagrams in which no Higgs is present. $A_{h/H}$ contain all VBS diagrams in which a h/H Higgs interacts with the vector bosons. They also contain a small set of additional diagrams, e.g. Higgsstrahlung ones. These can be ignored for all practical purposes since their contribution, with the present cut on the minimum invariant mass of the two jets which forbids them to resonate at the mass of a weak boson, is very small. From time to time we will refer to the sum of subamplitudes using the notation $A_{ij} = A_i + A_j$. A similar convention will be adopted for differential or total cross sections so that σ_i corresponds to the appropriate integral over phase space of $|A_i|^2$ summed over all contributing processes. As an example, σ_{0h} is obtained integrating the modulus squared of $A_{0h} = A_0 + A_h$, the coherent sum of the diagrams without any Higgs and those involving the light Higgs only.

The VBS diagrams in $A_{h/H}$ can be further classified by the pair of vector bosons which initiate the scattering and by the final state pair. In this paper we concentrate on $pp \to jjl^+l^-l'^+l'^-$ and $pp \to jjl^+\bar{\nu}_l l'^-\nu_{l'}$ production so that the only instances of VBS which appear correspond to $ZZ \to ZZ\,(Z2Z)$ and $WW \to ZZ\,(W2Z)$ for the $jjl^+l^-l'^+l'^-$ case and to $ZZ \to WW\,(Z2W)$ and $WW \to WW\,(W2W)$ for the $jjl^+\bar{\nu}_l l'^-\nu_{l'}$ final state.

The $W2Z$ and $Z2W$ sets are particularly simple because the Higgs fields appear only in the s-channel. In the $Z2Z$ case scalars are exchanged in the s-, t- and u-channel, while in the $W2W$ set the Higgses contribute in the s- and t-channel.

Some of the processes contributing to 4ljj production include only the $Z2Z$ subprocess, for instance $uc \to uc\,e^+e^-\mu^+\mu^-$; others only contain the $W2Z$ subprocess, for instance $us \to dc\,e^+e^-\mu^+\mu^-$. Finally there is a class of processes, like $ud \to ud\,e^+e^-\mu^+\mu^-$, which include both kind of subdiagrams. They will be called $P(Z2Z)$, $P(W2Z)$ and $P(Z2Z + W2Z)$ processes respectively.

Some processes leading to the 2l2νjj final state contain only the $Z2W$ set, for instance $u\bar{c} \to u\bar{c}\,e^+\bar{\nu}_e\mu^-\nu_\mu$; others only contain the $W2W$ set, like $u\bar{c} \to d\bar{s}\,e^+\bar{\nu}_e\mu^-\nu_\mu$. A third group of reactions includes both kind of subdiagrams, for instance $ud \to ud\,e^+\bar{\nu}_e\mu^-\nu_\mu$. They will be called $P(Z2W)$, $P(W2W)$ and $P(Z2W + W2W)$ processes, respectively.

The 4ljj final state has a tiny branching ratio but is very clean. The invariant mass of the leptonic system can be measured with high precision and small background.

In the 2l2νjj final state, the two charged leptons will be required to belong to different families and charges so that the final state can be thought of as containing a W^+W^- pair.

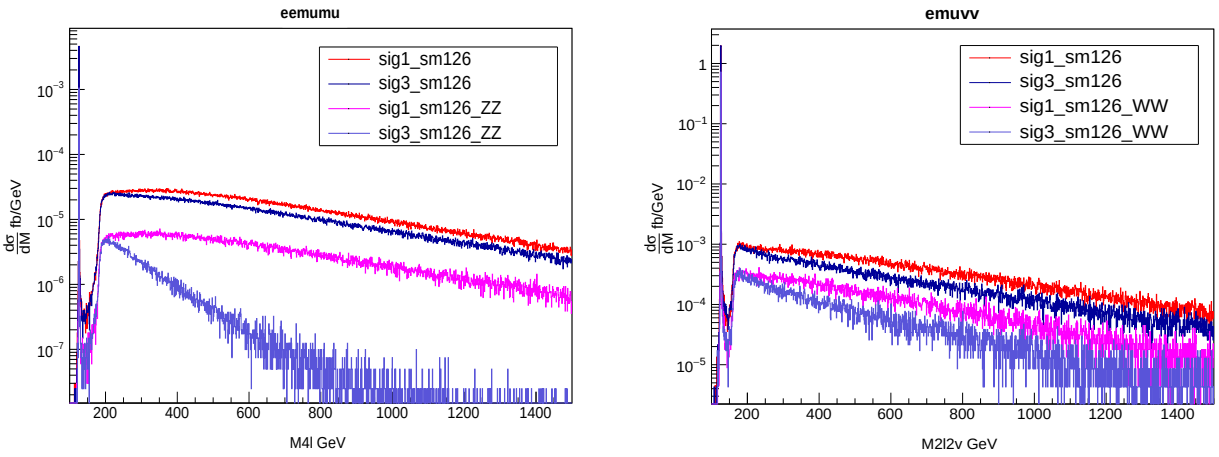

Figure 1. Invariant mass distribution of the four lepton system for the 4ljj final state (left) and the 2l2νjj final state (right) in the SM. In red and purple the mass distribution obtained taking into account only the diagrams with s-channel Higgs exchange and in blue and violet the result when the full set of Higgs exchange diagrams is included. On the left(right), the two contributions of the $P(Z2Z)(P(W2W))$ processes is shown separately.

The 2l2νjj final state has a much larger cross section. However, the invariant mass of the WW system cannot be reconstructed and it can only be experimentally analyzed in terms of the transverse mass of the leptonic system.

In the following we will examine these reactions with the aim of clarifying the role and size of interference effects in VBS, disregarding their actual observability at the LHC which would require a detailed study of all available channels and a careful assessment of reducible and irreducible backgrounds. Some of the distributions we present are not accessible in practice but are nonetheless useful tools for a first theoretical estimate of interference effects in different contexts.

We will begin our presentation with a discussion of the small set of diagrams in which VBS is mediated by Higgs exchange. The reason for this is the Caola-Melnikov approach to determining the Higgs width, which is based on a separation of the amplitude in a signal part, a background part and their interference. The three terms depend differently on the Higgs couplings, which are proportional to the Higgs width through the peak cross section. Varying these couplings within the experimental limits on off-shell ZZ and WW rates provides an upper bound on the Higgs total width. In Run II CMS and ATLAS plan to apply this procedure to Vector Boson Scattering and the set of diagrams in which VBS is mediated by Higgs exchange represents the signal term.

5 Higgs Mediated Vector Boson Scattering Signal in the SM

In fig. 1 we present results for the SM. On the left hand side we show in red the mass distribution for the 4ljj final state obtained taking into account only the diagrams with s-channel Higgs exchange and in blue the result when the full set of Higgs exchange diagrams is included. The contribution of the $P(Z2Z)$ processes is shown separately: in purple the

result due solely to s-channel Higgs exchange and in violet the result obtained from the sum of all three channels.

On the right hand side of fig. 1 we show the corresponding results for the 2l2νjj final state. In this case, it is the contribution of the $P(W2W)$ processes which is shown separately.

We see that there is a significant difference between the curves obtained considering only s-channel Higgs exchange and those obtained from the full set of scalar exchange diagrams. This implies a conspicuous negative interference between the Higgs exchange diagrams in $P(Z2Z)$ and $P(W2W)$ processes. This interference is so large that it significantly modifies the result obtained when all processes are summed, even though there are reactions which contribute substantially to the total which are not affected at all by these effects like $P(W2Z)$ and $P(Z2W)$ processes and others, the $P(Z2W + W2W)$ and $P(Z2Z + W2Z)$ groups, which are affected only partially.

Large cancellations in $P(Z2Z)$ processes are expected. On shell $ZZ \to ZZ$ scattering is zero in the absence of the Higgs and therefore does not violate unitarity at high energy. As a consequence the corresponding Higgs diagrams, each of which grows as the invariant mass squared of the process, must combine in such a way that their sum is actually asymptotically finite. At large energy, the longitudinal polarization vector of a Z boson of momentum p^μ can be identified with p^μ/M_Z and the sum of the three Feynman diagrams describing the scattering behaves as $s^2/s + t^2/t + u^2/u = s + t + u \approx 0$. It is however surprising that the cancellation grows very rapidly, above threshold, with the mass of the ZZ pair and becomes substantial already at moderate invariant masses. For $M_{ZZ} = 500$ GeV the square of the three Higgs exchange diagrams is an order of magnitude smaller than the result obtained from the s-channel exchange alone. The same cancellation takes place in the amplitude of the $P(Z2Z + W2Z)$ processes, while the $P(W2Z)$ sector is unaffected. In the sum of all processes the interference decreases the SM result for s-channel Higgs exchange by about 25%.

Interference effects are present also in $P(W2W)$ processes, as shown in the right hand side of fig. 1. They are less prominent than in the $P(Z2Z)$ case. The same cancellation takes place in the amplitude of the $P(Z2W + W2W)$ processes, while the $P(Z2W)$ sector is unaffected. Summing all processes, the difference between the result obtained from the single s-channel exchange diagram (red) and the full set (blue) is larger than for 4ljj production because WW initiated scatterings are more frequent than ZZ ones for the 2l2νjj final state. The interference decreases the SM result for s-channel Higgs exchange by about 30%. The on shell reaction $W^+W^- \to W^+W^-$ violates unitarity in a Higgsless theory when the W's are longitudinally polarized. Therefore Higgs exchange diagrams are necessary to restore unitarity and the cancellation can only be partial. There is no u-channel exchange, so, at large energy, the two diagrams behave as $t^2/t + s^2/s = t + s \approx -u$.

These results imply that, when producing Monte Carlo templates for the analysis of off shell Higgs production, it is mandatory to include the full set of Higgs exchange diagrams. This is in agreement with the Caola-Melnikov method which isolates terms in the amplitude which are proportional to the same power of the Higgs couplings. As a consequence all Higgs exchange diagrams need to be taken as a unit, regardless of the channel in which the

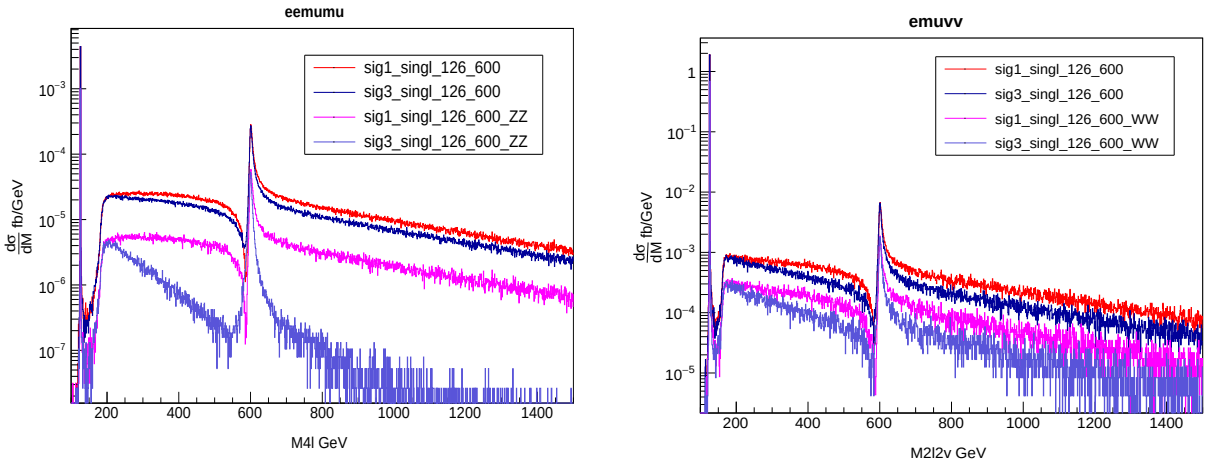

Figure 2. Invariant mass distribution of the four lepton system for the 4ljj final state (left) and the 2l2νjj final state (right) in the 1HSM with M_H= 600 GeV and $s_\alpha = 0.2$, $\tan\beta = 0.3$. In red and purple the mass distribution obtained taking into account only the diagrams with s-channel Higgs exchange and in blue and violet the result when the full set of Higgs exchange diagrams is included. On the left(right), the two contributions of the $P(Z2Z)(P(W2W))$ processes is shown separately.

exhange takes place. A production times decay approach is clearly inadequate to describe the off shell Higgs contribution. QCD radiative corrections in VBF are small. They are crucial in reducing the scale dependence of the predictions to the 5-10% level. NNLO corrections bring the uncertainty down to about 2%. When aiming for such an accuracy, interference effects, which have a comparable if not larger impact, cannot be ignored.

6 Higgs Mediated Vector Boson Scattering Signal in the 1HSM

We now turn to the 1HSM. We present results for selected values of M_H, s_α and $\tan\beta$ but our conclusions are fairly independent of the choice of parameters. In fig. 2 we show a number of four lepton mass distributions, for the 4ljj final state on the left and the 2l2νjj final state on the right, for $M_H = 600$ GeV, $s_\alpha = 0.2$ and $\tan\beta = 0.3$. The colors of the histograms in fig. 2 follow the convention of fig. 1. The red and purple lines refer to pure s-channel exchange. The red one relates to the sum of all processes while the purple one to $P(Z2Z)$ processes (left) and $P(W2W)$ ones (right), only. The blue and violet lines correspond to the sum of all Higgs exchange diagrams. The pattern and size of interference effects among different sets of Higgs exchange diagrams are similar to those in the SM. In addition, all curves in fig. 2, in the region around 600 GeV, show an interference pattern between the light and heavy Higgs similar to one present in the GGF case [9–12]. The inclusion of the full set of Higgs exchange diagrams decreases the size of the pure s-channel exchange amplitude over the whole energy range, as in the SM case, with the exception of a small region below the heavy Higgs mass where the interference between the two scalars dominate. It also significantly affects the interference pattern in the neighborhood of M_H.

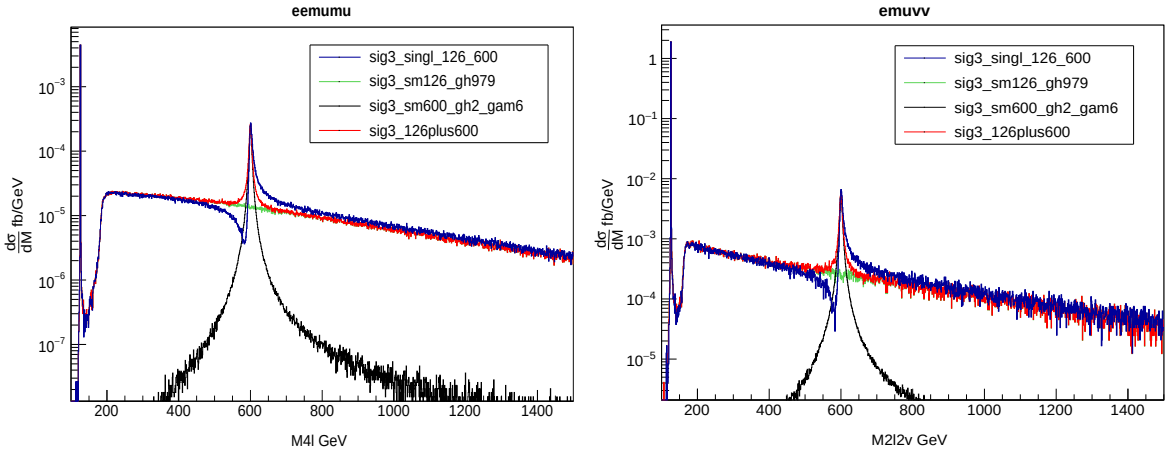

Figure 3. Invariant mass distribution of the four lepton system for the 4ljj final state in the 1HSM with M_H= 600 GeV and $s_\alpha = 0.2$, $\tan\beta = 0.3$. In green and black the mass distribution obtained taking into account the full set of Higgs exchange diagrams for Higgs masses of 125 and 600 GeV respectively. In red the incoherent sum of the two contributions. In blue the result of all Higgs diagrams in the 1HSM.

In fig. 3 we compare the invariant mass distribution of the four lepton system for the 4ljj (left) and 2l2νjj (right) final state obtained taking into account the full set of Higgs exchange diagrams in the 1HSM (blue) with the incoherent sum (red) of the Higgs exchange diagrams for Higgs masses of 125 and 600 GeV. The individual contributions of the two Higgs are shown in green and black respectively. The difference between the blue curve and the black and red ones illustrates the deformation of the Breit Wigner distribution induced by interference effects. They are negative in the region below M_H and positive above the heavy Higgs resonance as demonstraded by the comparison of the blue and red histograms. Effects are even larger if only the s-channel exchange is taken into account but from now on we only consider the full set of Higgs exchange diagrams which, even though not gauge invariant and therefore not physically observable, provides a better description of the Higgs contribution in the off shell region.

Clearly, this interference between different Higgs fields is not a peculiarity of the Singlet Model. It will indeed occur in any theory with multiple scalars which couple to the same set of elementary particles, albeit possibly with different strengths.

7 Full processes

After our presentation of the interplay of the different sets of Higgs exchange diagrams, we move to the discussion of the actual cross section for the production of a Singlet Model heavy Higgs at the LHC. The plot on the left hand side of fig. 4 shows the prediction for 4ljj production in the 1HSM (blue) with M_H= 600 GeV and $s_\alpha = 0.2$. Charged leptons satisfy the requirements in eq.(4.1) while jets pass the cuts in eq.(4.2). The 1HSM exact result is compared with different approximations. The green histograms is the light Higgs plus no-Higgs contribution, $d\sigma_{0h}/dM$; the red one refers to $d\sigma_{0H}/dM$; the gray one to

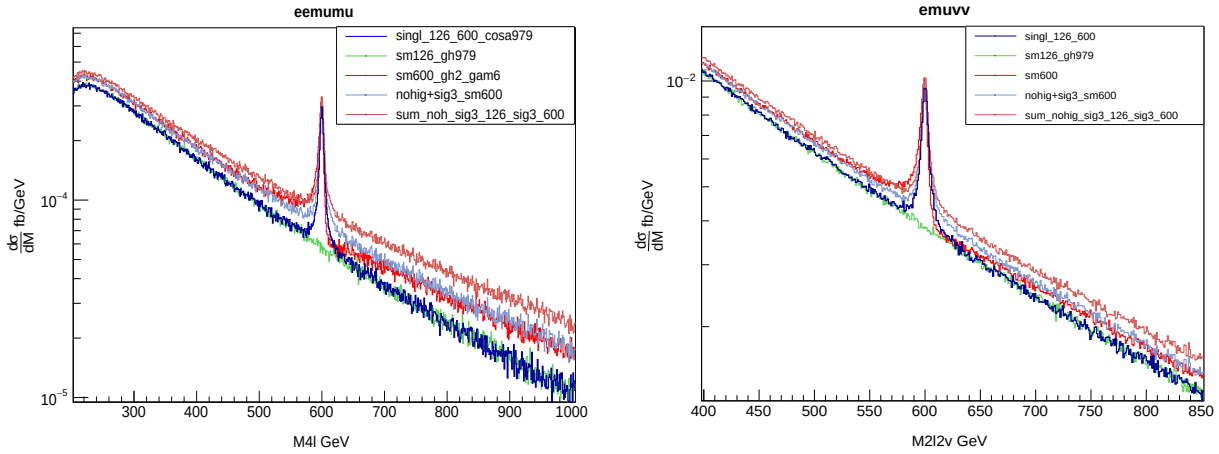

Figure 4. In blue, the invariant mass distribution of the four lepton system for the 4ljj final state (left) and the 2l2νjj final state (right) in the 1HSM with M_H= 600 GeV and $s_\alpha = 0.2$. The other curves are different approximations as detailed in the main text.

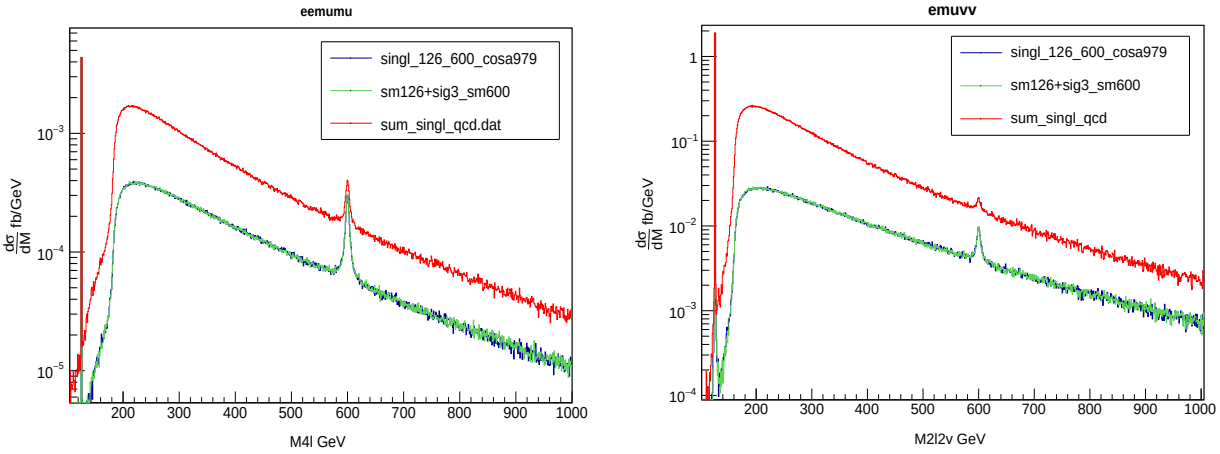

Figure 5. Invariant mass distribution of the four lepton system for the 4ljj final state (left) and the 2l2νjj final state (right) in the 1HSM with M_H= 600 GeV and $s_\alpha = 0.2$. The blue histogram is the exact 1HSM result. The green line refers to $d\sigma_{0h}/dM + d\sigma_H/dM$. The red curve is the sum of the 1HSM result and of the QCD contribution at $\mathcal{O}(\alpha_{EM}^4 \alpha_S^2)$.

$d\sigma_0/dM + d\sigma_H/dM$ and the brown one to $d\sigma_0/dM + d\sigma_h/dM + d\sigma_H/dM$. On the right hand side of fig. 4 the corresponding curves for the 2l2νjj final state are dispayed. None of the approximations in fig. 4 approaches the exact result better than about 20% in the region around the heavy scalar peak and they obviously fare even worse at large M_{4l}, with the exception of the green curve which misses only the heavy Higgs subamplitude, which is proportional to s_α^2 and numerically small in this energy range and outside the peak region, though necessary for unitarity. Clearly, neglecting any part of an amplitude requires a great deal of attention and a careful estimate of the resulting discrepancy.

There is however a combination of subamplitudes which provides a good approximation

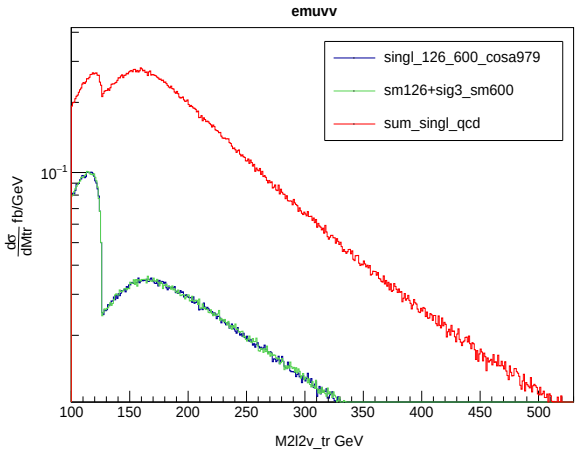

Figure 6. Transverse mass distribution of the four lepton system for the 2l2νjj final state in the 1HSM with M_H= 600 GeV and $s_\alpha = 0.2$. The blue histogram is the exact 1HSM result. The green line refers to $d\sigma_{0h}/dM + d\sigma_H/dM$. The red curve is the sum of the 1HSM result and of the QCD contribution at $\mathcal{O}(\alpha^4_{EM}\alpha^2_S)$.

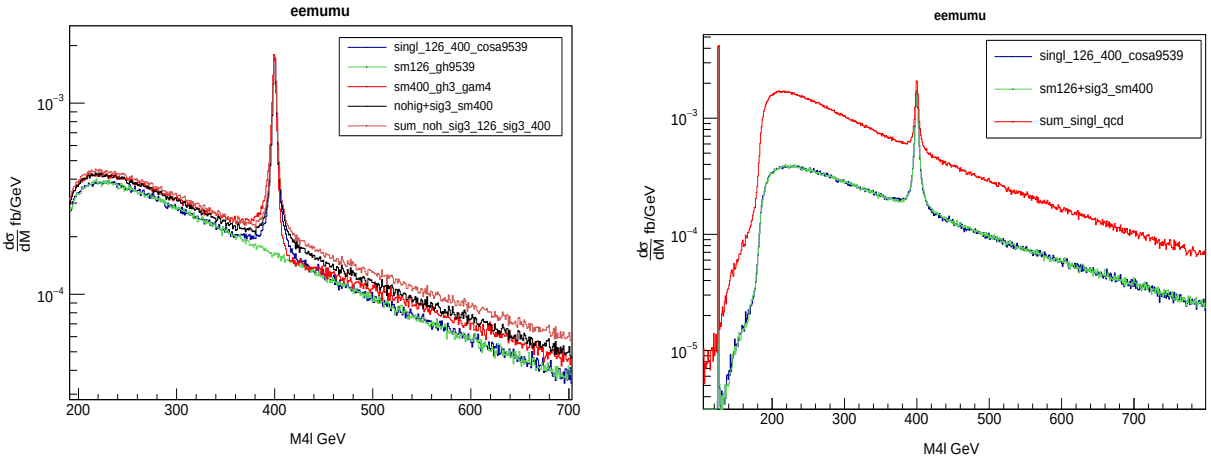

Figure 7. Invariant mass distribution of the four lepton system for the 4ljj final state in the 1HSM with M_H= 400 GeV, $s_\alpha = 0.3$ and $\tan\beta = 1.0$. On the left, the 1HSM result, in blue, is compared with different approximations as detailed in the main text. On the right the exact result is compared with $d\sigma_{0h}/dM + d\sigma_M/dM$,in green. The red curve is the sum of the 1HSM result and of the QCD contribution at $\mathcal{O}(\alpha^4_{EM}\alpha^2_S)$.

to the exact result. In fig. 5 the prediction for 4ljj/2l2νjj production in the 1HSM, in blue, is compared with the curve, in green, obtained from the incoherent sum of $d\sigma_{0h}/dM$ and $d\sigma_H/dM$, both of them computed with with 1HSM couplings and widths. The two histograms agree remarkably well over the full mass range. This is particularly meaningful in the region of the heavy Higgs peak where A_H is large: it implies that the interference terms of the heavy Higgs diagrams with A_h and A_0 cancel each other to a large degree. For comparison, we also show in red the sum of the full $\mathcal{O}(\alpha^6_{EM})$ result discussed above and

of the QCD contribution at $\mathcal{O}(\alpha_{EM}^4\alpha_S^2)$. The cross section is a factor of about three larger than the EW result.

As mentioned before, the invariant mass of the W boson pair is not measurable, therefore in fig. 6 we show the transverse mass distribution for the 2l2νjj final state. The transverse mass is defined as:

$$\left(M_T^{WW}\right)^2 = \left(E_{T,ll} + E_{T,miss}\right)^2 - |\vec{p}_{T,ll} + \vec{E}_{T,miss}|^2, \tag{7.1}$$

where $E_{T,ll} = \sqrt{(\vec{p}_{T,ll})^2 + M_{ll}^2}$. The heavy Higgs peak has been completely washed out, as expected. Also in this case, the sum $\sigma_{0h} + \sigma_H$ describes very well the exact distribution. Clearly the fully leptonic decay of the WW pair can only be considered as a case study. In order to employ the W^+W^-jj channel in the search for additional heavy scalars it will be necessary to consider the semileptonic decays.

As a check of the dependence of the effects discussed above on the heavy Higgs mass, in fig. 7 we show some results for 4ljj production in the 1HSM with M_H= 400 GeV, $s_\alpha = 0.3$ and $\tan\beta = 1.0$. On the left, the full result, in blue, is compared with different combinations of subamplitudes. The green histograms is the light Higgs plus no-Higgs contribution, $d\sigma_{0h}/dM$; the red one refers to $d\sigma_{0H}/dM$; the black one to $d\sigma_0/dM + d\sigma_H/dM$ and the brown one to $d\sigma_0/dM + d\sigma_h/dM + d\sigma_H/dM$. Again, none of these approximations describe satisfactoraly the region around the heavy scalar peak. All of them, with the exception of the green curve, lack terms which are crucial for the restoration of unitarity, and progressively diverge from the exact result as the four lepton mass increases. On the right the exact result is compared with $d\sigma_{0h}/dM + d\sigma_M/dM$. The agreement between two curves is impressive. In red we show the sum of the full $\mathcal{O}(\alpha_{EM}^6)$ result and of the QCD contribution at $\mathcal{O}(\alpha_{EM}^4\alpha_S^2)$.

8 Cancellation of the heavy Higgs interferences

It is noteworthy that the interference terms of the heavy Higgs diagrams with A_h and A_0 cancel each other almost exactly for different ranges of invariant mass of the final state vector boson pair and different small amount of mixing between the light and heavy Higgs. The interference corresponds to the real part of $A_H^* \times (A_0 + A_h)$. Since $A_h \propto c_\alpha^2$, the cancellation cannot take place for arbitrary values of of the mixing angle α.

In order to investigate further this phenomenon, in fig. 8 we isolate the interference term for different choices of parameters. In the upper row, the invariant mass distribution of the four lepton system for the 4l final state in the 1HSM with M_H= 600 GeV and $s_\alpha = 0.2$. In the lower row the corresponding plots for the 2l2νjj final state with M_H= 900 GeV and $s_\alpha = 0.4$, a rather extreme case in view of the allowed parameter space. Defining I_{ij} as the integrated interference between A_i and A_j, on the right we show $d\sigma_{hH}/dM - d\sigma_h/dM - d\sigma_H/dM = dI_{hH}/dM$ (red), $d\sigma_{H0}/dM - d\sigma_0/dM - d\sigma_H/dM = dI_{0H}/dM$ (violet) and $dI_{hH}/dM + dI_{0H}/dM$ (green). On the left we show $d\sigma_H/dM$ in blue, $d\sigma_H/dM + dI_{hH}/dM$ (red) and $d\sigma_H/dM + dI_{hH}/dM + dI_{0H}/dM$ (green).

The plot in the upper left corner shows how, for M_H= 600 GeV and $s_\alpha = 0.2$, the interference between the heavy and the light Higgs deforms the Breit-Wigner distribution

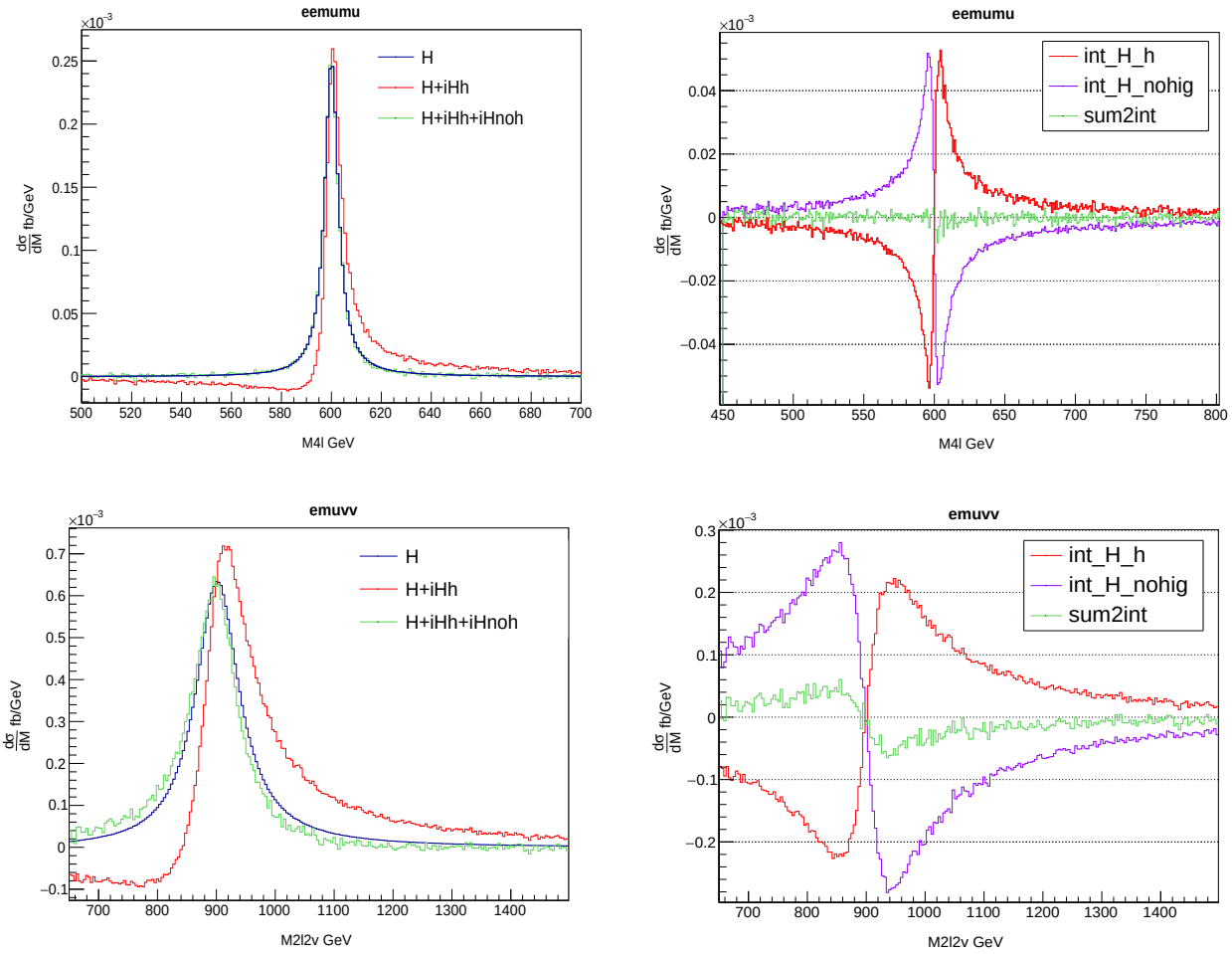

Figure 8. In the upper row, the invariant mass distribution of the four lepton system for the 4l final state in the 1HSM with M_H= 600 GeV and $s_\alpha = 0.2$. In the lower row the corresponding plots for the 2l2νjj final state with M_H= 900 GeV and $s_\alpha = 0.4$. On the left we show $d\sigma_H/dM$ (blue), $d\sigma_H/dM + dI_{hH}/dM$ (red) and $d\sigma_H/dM + dI_{hH}/dM + dI_{0H}/dM$ (green). On the right we show dI_{hH}/dM (red), dI_{0H}/dM (violet) and $dI_{hH}/dM + dI_{0H}/dM$ (green).

of the heavy scalar and how the inclusion of the interference between the heavy Higgs and the subamplitude without any Higgs pratically eliminates the deformation. The plot on the top right displays the two interferences and their sum, which is zero within statistical uncertainty. The two plots in the lower part provide the same information for the 2l2νjj final state with M_H= 900 GeV and $s_\alpha = 0.4$. Since now $c_\alpha^2 = 0.84$ is larger than in the previous example, the interference between the heavy scalar and the noHiggs amplitude is larger in absolute value than the interference between the two Higgs. As a consequence the sum is non zero and agrees in sign with the former of the two interferences but, as already mentioned, for parameters outside their allowed range.

The vector bosons in the heavy Higgs decay, for all the masses we have considered, are predominantly longitudinally polarized. In order to preserve unitarity the leading term of the contributions to jjV_LV_L production from vector boson interactions and from Higgs

	200 GeV $< M_{4l} <$ 1 TeV				$\lvert M_{4l} - M_H \rvert <$ 25 GeV			
M_H (GeV), s_α	σ	σ_{0h}	σ_{0h}+σ_H	σ_{SM}	σ	σ_{0h}	σ_{0h}+σ_H	σ_{SM}
400, 0.3, 4l	98.1	87.4	98.2	86.9	18.3	8.1	18.3	8.1
600, 0.2, 4l	89.4	87.0	89.5	86.9	5.2	2.9	5.3	2.9
600, 0.2, 2l2ν	5931	5870	5931	5874	248	193	253	192

Table 1. Cross sections in ab at the LHC with a center of mass energy of 13 TeV. σ_{SM} corresponds to $s_\alpha = 0$. The SM cross section in $|M_{4l} - M_H| < 25$ GeV can be considered as the SM background to the heavy Higgs.

exchange must cancel each other exactly in the large energy limit, where vector and Higgs masses can be neglected. The near perfect suppression we observe between A_0 and A_h, which results in a small interference of the heavy Higgs with the rest of the amplitude, suggests that the cancellation between A_0 and A_h sets in already for invariant masses of the vector pair of a few hundred GeV, provided the mixing angle is not too large.

Similar analysis have been performed for the GGF case in ref. [11], highlighting a partial cancellation between the interferences of the Heavy Higgs with the light one and with the continuum.

In tab. 1 we show the cross section in attobarns for two mass intervals: 200 GeV $< M_{4l} <$ 1 TeV, which roughly coincides with the range employed so far by the experimental collaborations to set limits on the presence and couplings of additional scalars, and $|M_{4l} - M_H| < 25$ GeV, as an indication of the possible effects on an analysis in smaller mass bins which requires high luminosity. The corresponding cross sections for the $\mathcal{O}(\alpha_{EM}^4 \alpha_S^2)$ 4l processes are 222 ab in the 200 GeV-1 TeV interval, 18.4 ab in the 375 GeV-425 GeV range, 5.4 ab in the 575 GeV-625 GeV range. For the 2l2νjj final state the $\mathcal{O}(\alpha_{EM}^4 \alpha_S^2)$ cross sections are 30 fb between 200 GeV and 1 TeV, and 580 ab in the 575 GeV-625 GeV interval.

We notice that $\sigma_{0h} \approx \sigma_{SM}(s_\alpha = 0)$ in both intervals. The only difference between the two results is that in the first case the Higgs couplings are scaled by c_α. Therefore, the off shell predictions are hardly affected by this modification.

The incoherent sum σ_{0h}+σ_H agrees with the exact result in all cases also when integrated over.

Even in the smaller interval σ_{0h} gives a substantial contribution to VV production and must be taken into account when searching for a heavy Higgs.

9 Conclusions

We have studied Higgs sector interference effects in Vector Boson Scattering at the LHC, both in the Standard Model and its one Higgs Singlet extension as a prototype of theories in which more than one neutral, $\mathcal{CP}$ even, scalars are present. We have concentrated on $pp \to jj\, l^+ l^- l'^+ l'^-$ and $pp \to jj\, l^+ \bar{\nu}_l l'^- \nu_{l'}$ production. We have shown that large interferences among the different Higgs exchange channels are present in the SM and that a production times decay approach fails to reproduce the off shell Higgs contribution.

In the 1HSM, there are additional interferences between the two Higgs fields. Different approximations have been tried and proved inaccurate. We have found that the interference between the heavy Higgs diagrams and the rest of the amplitude, which is the sum of light Higgs exchange diagrams and of those diagrams in which no Higgs appear, is very small for values of the mixing angle compatible with the experimental constraints and can be neglected.

Acknowledgments

Several stimulating discussions with Anna Kropivnitskaya and Pietro Govoni are gratefully acknowledged. This work has been supported by MIUR (Italy) under contract 2010YJ2NYW_006, by the Compagnia di San Paolo under contract ORTO11TPXK and by the European Union Initial Training Network HiggsTools (PITN-GA-2012-316704).

References

[1] **ATLAS** Collaboration, G. Aad et al., *Observation of a new particle in the search for the Standard Model Higgs boson with the ATLAS detector at the LHC*, *Phys.Lett.* **B716** (2012) 1–29, [arXiv:1207.7214].

[2] **CMS** Collaboration, S. Chatrchyan et al., *Observation of a new boson at a mass of 125 GeV with the CMS experiment at the LHC*, *Phys.Lett.* **B716** (2012) 30–61, [arXiv:1207.7235].

[3] **CMS** Collaboration, V. Khachatryan et al., *Precise determination of the mass of the Higgs boson and tests of compatibility of its couplings with the standard model predictions using proton collisions at 7 and 8 TeV*, *Eur.Phys.J.* **C75** (2015), no. 5 212, [arXiv:1412.8662].

[4] **ATLAS, CMS** Collaboration, G. Aad et al., *Combined Measurement of the Higgs Boson Mass in pp Collisions at $\sqrt{s} = 7$ and 8 TeV with the ATLAS and CMS Experiments*, *Phys.Rev.Lett.* **114** (2015) 191803, [arXiv:1503.07589].

[5] **ATLAS** Collaboration, "Updated coupling measurements of the Higgs boson with the ATLAS detector using up to 25 fb^{-1} of proton-proton collision data." ATLAS-CONF-2014-009, ATLAS-COM-CONF-2014-013, 2014.

[6] **ATLAS** Collaboration, "Constraints on New Phenomena via Higgs Coupling Measurements with the ATLAS Detector." ATLAS-CONF-2014-010, ATLAS-COM-CONF-2014-011, 2014.

[7] **CMS** Collaboration, "Searches for new processes in the scalar sector at the CMS experiment." CMS CR-2014/091, 2014.

[8] F. Caola and K. Melnikov, *Constraining the Higgs boson width with ZZ production at the LHC*, *Phys.Rev.* **D88** (2013) 054024, [arXiv:1307.4935].

[9] C. Englert, Y. Soreq, and M. Spannowsky, *Off-Shell Higgs Coupling Measurements in BSM scenarios*, arXiv:1410.5440.

[10] E. Maina, *Interference effects in Heavy Higgs production via gluon fusion in the Singlet Extension of the Standard Model*, arXiv:1501.02139.

[11] N. Kauer and C. O'Brien, *Heavy Higgs signal-background interference in $gg \to VV$ in the Standard Model plus real singlet*, arXiv:1502.04113.

[12] C. Englert, I. Low, and M. Spannowsky, *On-shell interference effects in Higgs boson final states*, *Phys.Rev.* **D91** (2015), no. 7 074029, [arXiv:1502.04678].

[13] C. Englert and M. Spannowsky, *Limitations and Opportunities of Off-Shell Coupling Measurements*, *Phys.Rev.* **D90** (2014), no. 5 053003, [arXiv:1405.0285].

[14] M. Ciccolini, A. Denner, and S. Dittmaier, *Strong and electroweak corrections to the production of Higgs + 2jets via weak interactions at the LHC*, *Phys.Rev.Lett.* **99** (2007) 161803, [arXiv:0707.0381].

[15] M. Ciccolini, A. Denner, and S. Dittmaier, *Electroweak and QCD corrections to Higgs production via vector-boson fusion at the LHC*, *Phys.Rev.* **D77** (2008) 013002, [arXiv:0710.4749].

[16] P. Bolzoni, F. Maltoni, S.-O. Moch, and M. Zaro, *Higgs production via vector-boson fusion at NNLO in QCD*, *Phys.Rev.Lett.* **105** (2010) 011801, [arXiv:1003.4451].

[17] P. Bolzoni, F. Maltoni, S.-O. Moch, and M. Zaro, *Vector boson fusion at NNLO in QCD: SM Higgs and beyond*, *Phys.Rev.* **D85** (2012) 035002, [arXiv:1109.3717].

[18] V. Silveira and A. Zee, *Scalar Phantoms*, *Phys.Lett.* **B161** (1985) 136.

[19] R. Schabinger and J. D. Wells, *A Minimal spontaneously broken hidden sector and its impact on Higgs boson physics at the large hadron collider*, *Phys.Rev.* **D72** (2005) 093007, [hep-ph/0509209].

[20] D. O'Connell, M. J. Ramsey-Musolf, and M. B. Wise, *Minimal Extension of the Standard Model Scalar Sector*, *Phys.Rev.* **D75** (2007) 037701, [hep-ph/0611014].

[21] O. Bahat-Treidel, Y. Grossman, and Y. Rozen, *Hiding the Higgs at the LHC*, *JHEP* **0705** (2007) 022, [hep-ph/0611162].

[22] V. Barger, P. Langacker, M. McCaskey, M. J. Ramsey-Musolf, and G. Shaughnessy, *LHC Phenomenology of an Extended Standard Model with a Real Scalar Singlet*, *Phys.Rev.* **D77** (2008) 035005, [arXiv:0706.4311].

[23] G. Bhattacharyya, G. C. Branco, and S. Nandi, *Universal Doublet-Singlet Higgs Couplings and phenomenology at the CERN Large Hadron Collider*, *Phys.Rev.* **D77** (2008) 117701, [arXiv:0712.2693].

[24] M. Gonderinger, Y. Li, H. Patel, and M. J. Ramsey-Musolf, *Vacuum Stability, Perturbativity, and Scalar Singlet Dark Matter*, *JHEP* **1001** (2010) 053, [arXiv:0910.3167].

[25] S. Dawson and W. Yan, *Hiding the Higgs Boson with Multiple Scalars*, *Phys.Rev.* **D79** (2009) 095002, [arXiv:0904.2005].

[26] S. Bock, R. Lafaye, T. Plehn, M. Rauch, D. Zerwas, et al., *Measuring Hidden Higgs and Strongly-Interacting Higgs Scenarios*, *Phys.Lett.* **B694** (2010) 44–53, [arXiv:1007.2645].

[27] P. J. Fox, D. Tucker-Smith, and N. Weiner, *Higgs friends and counterfeits at hadron colliders*, *JHEP* **1106** (2011) 127, [arXiv:1104.5450].

[28] C. Englert, T. Plehn, D. Zerwas, and P. M. Zerwas, *Exploring the Higgs portal*, *Phys.Lett.* **B703** (2011) 298–305, [arXiv:1106.3097].

[29] C. Englert, J. Jaeckel, E. Re, and M. Spannowsky, *Evasive Higgs Maneuvers at the LHC*, *Phys.Rev.* **D85** (2012) 035008, [arXiv:1111.1719].

[30] B. Batell, S. Gori, and L.-T. Wang, *Exploring the Higgs Portal with 10/fb at the LHC*, *JHEP* **1206** (2012) 172, [arXiv:1112.5180].

[31] C. Englert, T. Plehn, M. Rauch, D. Zerwas, and P. M. Zerwas, *LHC: Standard Higgs and Hidden Higgs*, *Phys.Lett.* **B707** (2012) 512–516, [arXiv:1112.3007].

[32] R. S. Gupta and J. D. Wells, *Higgs boson search significance deformations due to mixed-in scalars*, *Phys.Lett.* **B710** (2012) 154–158, [arXiv:1110.0824].

[33] B. Batell, D. McKeen, and M. Pospelov, *Singlet Neighbors of the Higgs Boson*, *JHEP* **1210** (2012) 104, [arXiv:1207.6252].

[34] J. M. No and M. Ramsey-Musolf, *Probing the Higgs Portal at the LHC Through Resonant di-Higgs Production*, *Phys.Rev.* **D89** (2014), no. 9 095031, [arXiv:1310.6035].

[35] G. M. Pruna and T. Robens, *The Higgs Singlet extension parameter space in the light of the LHC discovery*, *Phys.Rev.* **D88** (2013) 115012, [arXiv:1303.1150].

[36] D. Lpez-Val and T. Robens, *r and the W-boson mass in the singlet extension of the standard model*, *Phys.Rev.* **D90** (2014), no. 11 114018, [arXiv:1406.1043].

[37] S. Profumo, M. J. Ramsey-Musolf, C. L. Wainwright, and P. Winslow, *Singlet-catalyzed electroweak phase transitions and precision Higgs boson studies*, *Phys.Rev.* **D91** (2015), no. 3 035018, [arXiv:1407.5342].

[38] C.-Y. Chen, S. Dawson, and I. Lewis, *Exploring resonant di-Higgs boson production in the Higgs singlet model*, *Phys.Rev.* **D91** (2015), no. 3 035015, [arXiv:1410.5488].

[39] T. Robens and T. Stefaniak, *Status of the Higgs Singlet Extension of the Standard Model after LHC Run 1*, *Eur.Phys.J.* **C75** (2015), no. 3 104, [arXiv:1501.02234].

[40] H. E. Logan, *Hiding a Higgs width enhancement from off-shell gg ($\rightarrow$ h*) $\rightarrow$ ZZ*, arXiv:1412.7577.

[41] A. Falkowski, C. Gross, and O. Lebedev, *A second Higgs from the Higgs portal*, *JHEP* **1505** (2015) 057, [arXiv:1502.01361].

[42] A. Ballestrero, A. Belhouari, G. Bevilacqua, V. Kashkan, and E. Maina, *PHANTOM: A Monte Carlo event generator for six parton final states at high energy colliders*, *Comput.Phys.Commun.* **180** (2009) 401–417, [arXiv:0801.3359].

[43] A. Ballestrero, D. B. Franzosi, and E. Maina, *Vector-Vector scattering at the LHC with two charged leptons and two neutrinos in the final state*, *JHEP* **1106** (2011) 013, [arXiv:1011.1514].

[44] J. M. Campbell and R. K. Ellis, *Higgs constraints from vector boson fusion and scattering*, *JHEP* **1504** (2015) 030, [arXiv:1502.02990].

[45] N. D. Christensen and C. Duhr, *FeynRules - Feynman rules made easy*, *Comput.Phys.Commun.* **180** (2009) 1614–1641, [arXiv:0806.4194].

[46] A. Alloul, N. D. Christensen, C. Degrande, C. Duhr, and B. Fuks, *FeynRules 2.0 - A complete toolbox for tree-level phenomenology*, *Comput.Phys.Commun.* **185** (2014) 2250–2300, [arXiv:1310.1921].

[47] C. Degrande, C. Duhr, B. Fuks, D. Grellscheid, O. Mattelaer, et al., *UFO - The Universal FeynRules Output*, *Comput.Phys.Commun.* **183** (2012) 1201–1214, [arXiv:1108.2040].

[48] Y. Zeldovich, I. Y. Kobzarev, and L. Okun, *Cosmological Consequences of the Spontaneous Breakdown of Discrete Symmetry*, *Zh.Eksp.Teor.Fiz.* **67** (1974) 3–11.

[49] T. Kibble, *Topology of Cosmic Domains and Strings*, *J.Phys.* **A9** (1976) 1387–1398.

[50] T. Kibble, *Some Implications of a Cosmological Phase Transition*, *Phys.Rept.* **67** (1980) 183.

[51] S. Abel, S. Sarkar, and P. White, *On the cosmological domain wall problem for the minimally extended supersymmetric standard model*, *Nucl.Phys.* **B454** (1995) 663–684, [hep-ph/9506359].

[52] A. Friedland, H. Murayama, and M. Perelstein, *Domain walls as dark energy*, *Phys.Rev.* **D67** (2003) 043519, [astro-ph/0205520].

[53] V. Barger, P. Langacker, M. McCaskey, M. Ramsey-Musolf, and G. Shaughnessy, *Complex Singlet Extension of the Standard Model*, *Phys.Rev.* **D79** (2009) 015018, [arXiv:0811.0393].

[54] **LHC Higgs Cross Section Working Group** Collaboration, S. Heinemeyer et al., *Handbook of LHC Higgs Cross Sections: 3. Higgs Properties*, arXiv:1307.1347.

[55] J. Pumplin, D. Stump, J. Huston, H. Lai, P. M. Nadolsky, et al., *New generation of parton distributions with uncertainties from global QCD analysis*, *JHEP* **0207** (2002) 012, [hep-ph/0201195].